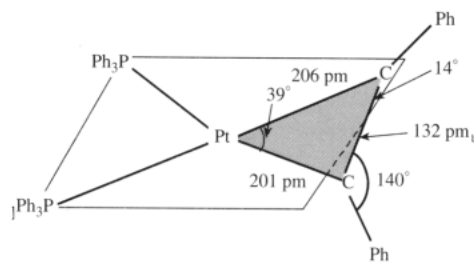
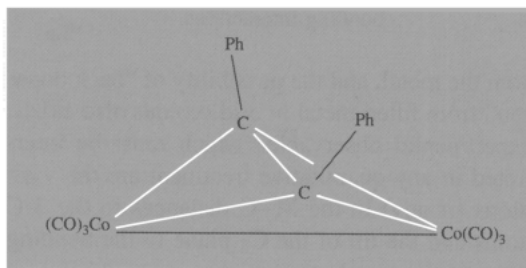


**Figure 19.21** Structure of  $[\text{Pt}(\eta^2\text{-C}_2\text{Bu}'_2)\text{Cl}_2(4\text{-toluidine})]$ .



**Figure 19.22** Structure of  $[\text{Pt}(\eta^2\text{-C}_2\text{Ph}_2)(\text{PPh}_3)_2]$ .

The classic example is  $[\text{Co}_2(\text{CO})_6(\text{C}_2\text{Ph}_2)]$  which is formed by direct displacement of the 2 bridging carbonyls in  $[\text{Co}_2(\text{CO})_8]$  to give the structure sketched below:



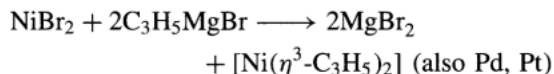
The C–C group lies above and at right angles to the Co–Co vector; the C–C distance is 146 pm (27 pm greater than in the free alkyne) and this has been taken to indicate extensive back donation from the 2 Co atoms. The Co–Co distance is 247 pm compared with 252 pm in  $\text{Co}_2(\text{CO})_8$ . A rather different situation is found in  $[\text{Ru}_4(\mu_4\text{-}\eta^1, \eta^2\text{-C}_2)(\mu\text{-PPh}_2)_2(\text{CO})_{12}]$ , where a  $\mu_4\text{-}\eta^1, \eta^2\text{-acetylide}$  dianion bridges two  $\{\text{Ru}_2(\mu\text{-PPh}_2)(\text{CO})_6\}$  units. Here, the steric demands of the other ligands make the C–C bridge almost coplanar with the two  $\eta^2$ -bonded

Ru atoms, and reduced  $\pi$ -bonding is indicated by a much shorter (127.5 pm) C–C distance.<sup>(38a)</sup>

### 19.7.3 Trihapto ligands

The possibility that the allyl group  $\text{CH}_2=\text{CH}-\text{CH}_2-$  can act as an  $\eta^3$  ligand was recognized independently by several groups in 1960 and since then the field has flourished, partly because of its importance in homogeneous catalysis and partly because of the novel steric possibilities and interconversions that can be studied by proton nmr spectroscopy. Many synthetic routes are available of which the following are representative.

(a) Allyl Grignard reagent:

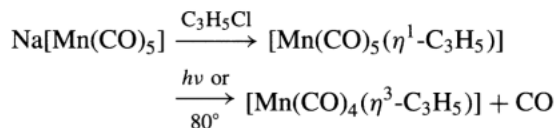


A mixture of *cis* and *trans* isomers is obtained:



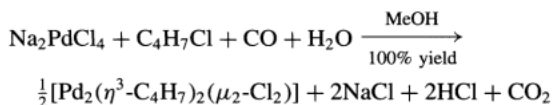
*Tris*-( $\eta^3$ -allyl) complexes  $[\text{M}(\text{C}_3\text{H}_5)_3]$  can be prepared similarly for V, Cr, Fe, Co, Rh, Ir, and *tetrakis* complexes  $[\text{M}(\eta^3\text{-C}_3\text{H}_5)_4]$  for Zr, Th, Mo and W.

(b) Conversion of  $\eta^1$ -allyl to  $\eta^3$ -allyl:



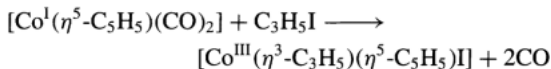
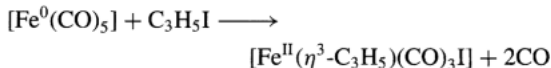
Similarly many other  $\eta^1$ -allyl carbonyl complexes convert to  $\eta^3$ -allyl complexes with loss of 1 CO.

(c) From allylic halides (e.g. 2-methylallyl chloride):

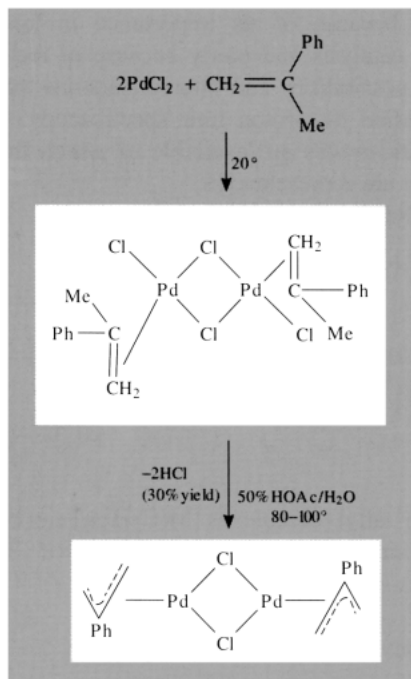


<sup>38a</sup> M. I. BRUCE, M. R. SNOW, E. R. T. TIEKINK and M. L. WILLIAMS, *J. Chem. Soc., Chem. Commun.*, 701-2 (1986).

(d) Oxidative addition of allyl halides, e.g.:



(e) Elimination of HCl from an alkene metal halide complex, e.g.:



The bonding in  $\eta^3$ -allylic complexes can be described in terms of the qualitative MO theory illustrated in Fig. 19.23. The  $p_z$  orbitals on the 3 allylic C atoms can be combined to give the 3 orbitals shown in the upper part of Fig. 19.23; each retains  $\pi$  symmetry with respect to the  $C_3$  plane but has, in addition, 0, 1 or 2 nodes perpendicular to this plane. The metal orbitals of appropriate symmetry to form bonding MOs with these 3 combinations are shown in the lower part of Fig. 19.23. The extent to which these orbitals are, in fact, involved in bonding depends on their relative energies, their radial diffuseness and the actual extent of orbital overlap. Electrons to fill these bonding MOs can be thought of as coming both from the allylic  $\pi$ -electron cloud and

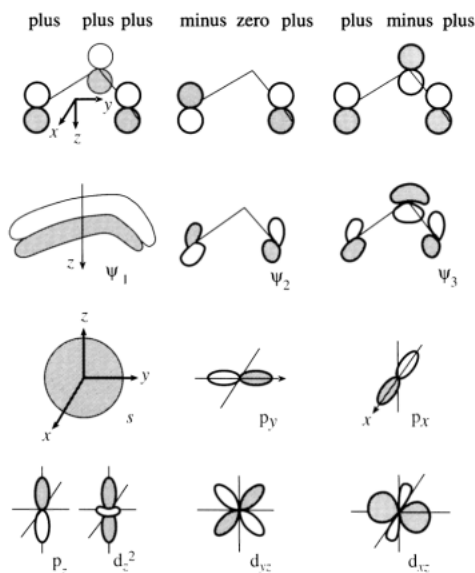


**Figure 19.23** Schematic illustration of possible combinations of orbitals in the  $\pi$ -allylic complexes. The bonding direction is taken to be the  $z$ -axis with the M atom below the  $C_3$  plane. Appropriate combinations of  $p_\pi$  orbitals on the 3 C are shown in the top half of the figure, and beneath them are the metal orbitals with which they are most likely to form bonding interactions.

from the metal, and the possibility of “back donation” from filled metal hybrid orbitals also exists. Experimental observables which must be interpreted in any quantitative treatment are the variations (if any) in the M–C distances to the 3 C atoms and the tilt of the  $C_3$  plane to the bonding plane of the metal atom.

In addition to acting as an  $\eta^1$  and an  $\eta^3$  ligand the allyl group can also act as a bridging ligand by  $\eta^1$  bonding to one metal atom and  $\eta^2$  bonding via the alkene function to a second metal atom. For example  $[\text{Pt}_2(\text{acac})_2(\eta^1, \eta^2\text{-C}_3\text{H}_5)_2]$  has the dimeric structure shown in Fig. 19.24. The compound was made from  $[\text{Pt}(\eta^3\text{-C}_3\text{H}_5)_2]$  by treatment first with HCl to give polymeric  $[\text{Pt}(\text{C}_3\text{H}_5)\text{Cl}]$  and then with thallium(I) acetylacetonate.

Many  $\eta^3$ -allyl complexes are fluxional (p. 914) at room temperature or slightly above,

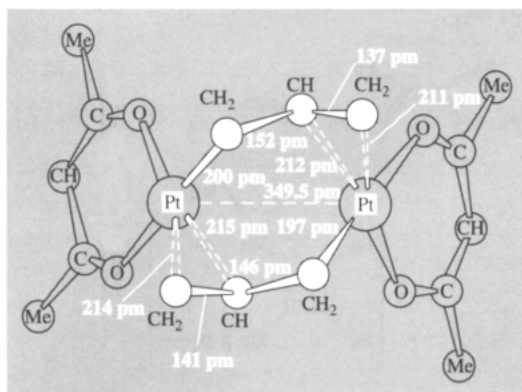
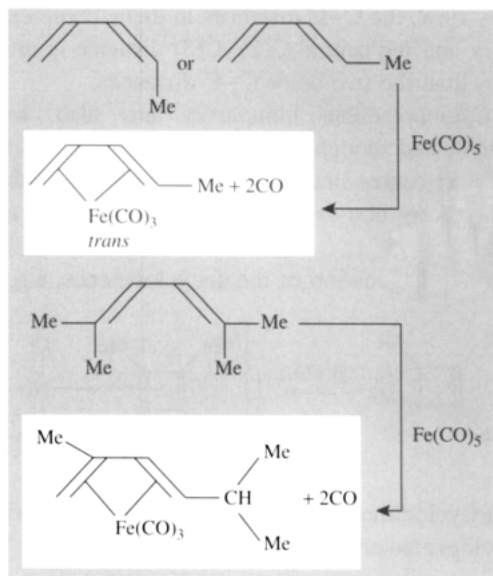


**Figure 19.24** Structure of  $[\text{Pt}_2(\text{acac})_2(\mu\text{-C}_3\text{H}_5)_2]$  showing the bridging allyl groups, each  $\eta^1$  bonded to 1 Pt and  $\eta^2$ -bonded to the other. Interatomic distances are in pm with standard deviations of  $\sim 5$  pm for Pt–C and  $\sim 7$  for C–C. The distance of Pt to the centre of the  $\eta^2$ -C<sub>2</sub> group is 201 pm, very close to the  $\eta^1$ -Pt–C distance of 199 pm.

and this property has been extensively studied by  $^1\text{H}$  nmr spectroscopy. Exceedingly complex patterns can emerge. The simplest interchange that can occur is between those H atoms which are on the side nearer the metal (*syn*) and those which are on the side away from the metal (*anti*) probably via a short-lived  $\eta^1$ -allyl metal intermediate. The fluxional behaviour can be slowed down by lowering the temperature, and separate resonances from the various types of H atom are then observed. Fluxionality can also sometimes be quenched by incorporating the allylic group in a ring system which restricts its mobility.

### 19.7.4 Tetrahapto ligands

Conjugated dienes such as butadiene and its open-chain analogues can act as  $\eta^4$  ligands; the complexes are usually prepared from metal carbonyl complexes by direct replacement of 2CO by the diene. Isomerization or rearrangement of the diene may occur as indicated schematically below:



No new principles are involved in describing the bonding in these complexes and appropriate combinations of the  $4p_\pi$  orbitals on the diene system can be used to construct MOs with the metal-based orbitals for donation and back donation of electron density.<sup>(39)</sup> As with ethene, two limiting cases can be envisaged which can be represented schematically as in Fig. 19.25. Consistent with

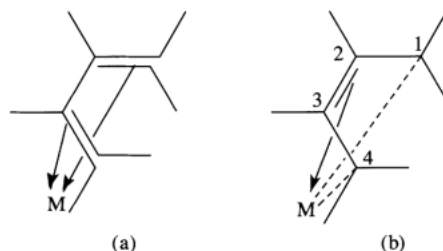


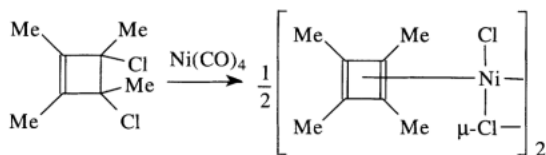
**Figure 19.25** Schematic representation of the two formal extremes of bonding in 1,3-diene complexes. In (a) the bonding is considered as two almost independent  $\eta^2$ -alkene-metal bonds, whereas in (b) there are  $\sigma$  bonds to C(1) and C(4) and an  $\eta^2$ -alkene-metal bond from C(2)–C(3).

<sup>39</sup> D. M. P. MINGOS, *J. Chem. Soc., Dalton Trans.*, 20–35 (1977).

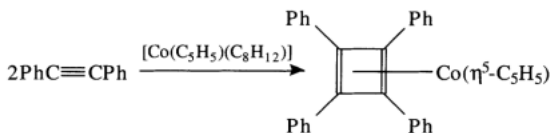
this view, the C–C distances in diene complexes vary and the central C(2)–C(3) distance is often less than the two outer C–C distances.

Cyclobutadiene complexes are also well established though they must be synthesized by indirect routes since the parent dienes are either unstable or non-existent. Four general routes are available:

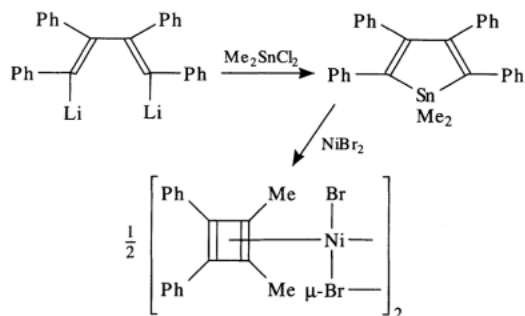
(a) Dehalogenation of dihalocyclobutenes, e.g.:



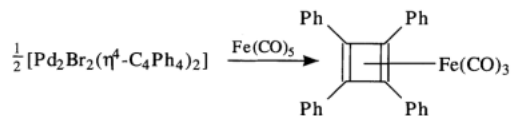
(b) Cyclodimerization of alkynes, e.g. with cyclopentadienyl-(cycloocta-1,5-diene)cobalt:



(c) From metallacyclopentadienes:



(d) Ligand exchange from other cyclobutadiene complexes, e.g.:



A schematic interpretation of the bonding in cyclobutadiene complexes can be given within the framework outlined in the preceding sections and this is illustrated in Fig. 19.26.

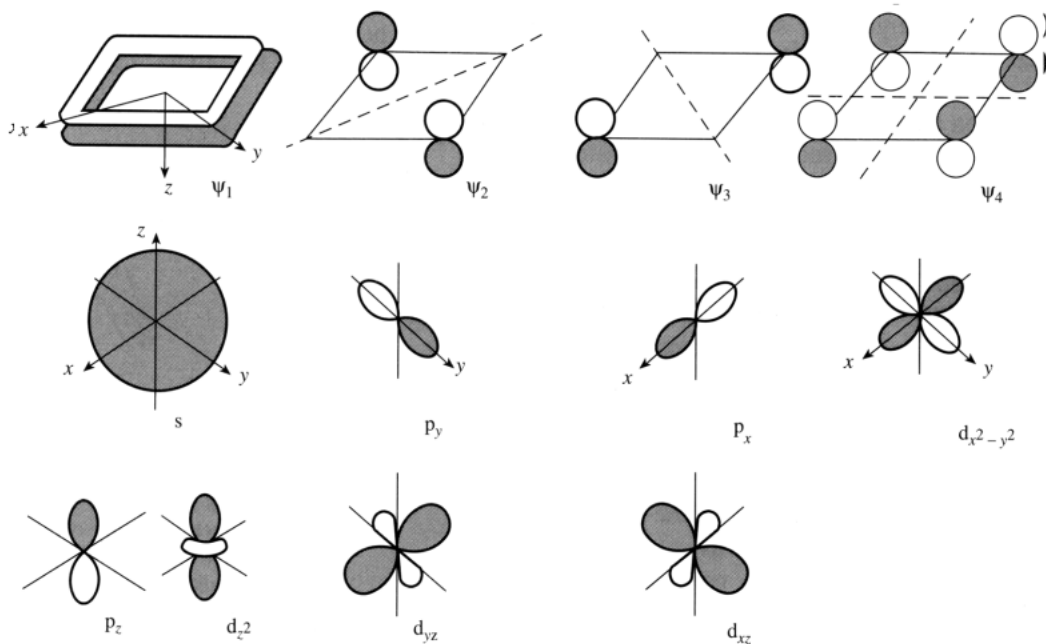


**Figure 19.26** Orbitals used in describing the bonding in metal- $\eta^2$ -cyclobutadiene complexes. The sign convention and axes are as in Fig. 19.23.

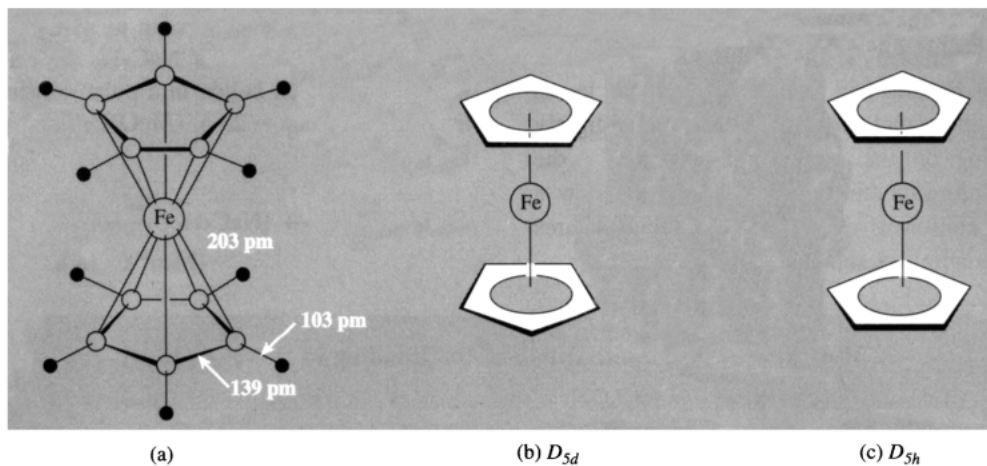


**Figure 19.27** Structure of ferrocene,  $[\text{Fe}(\eta^5\text{-C}_5\text{H}_5)_2]$ , and a conventional “shorthand” representation.

Cyclobutadiene complexes afford a classic example of the stabilization of a ligand by coordination to a metal and, indeed, were predicted theoretically on this basis by H. C. Longuet-Higgins and L. E. Orgel (1956) some 3 y before the first examples were synthesized. In the (hypothetical) free cyclobutadiene molecule 2 of the 4  $\pi$ -electrons would occupy  $\psi_1$  and there would be an unpaired electron in each of the 2 degenerate orbitals  $\psi_2$ ,  $\psi_3$ . Coordination to a metal provides further interactions and avoids this unstable configuration. See also the discussion on ferrocenes (p. 174).

### 19.7.5 Pentahapto ligands

The importance of bis(cyclopentadienyl)iron  $[\text{Fe}(\eta^5\text{-C}_5\text{H}_5)_2]$  in the development of organometallic chemistry has already been alluded to (p. 924). The compound, which forms orange crystals, mp  $174^\circ$ , has extraordinary thermal stability ( $>500^\circ$ ) and a remarkable structure which was unique when first established. It also has an extensive aromatic-type reaction chemistry which is reflected in its common name “ferrocene”. The molecular structure of ferrocene in the crystalline state features two parallel cyclopentadienyl rings: at one time these

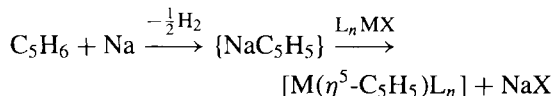
rings were thought to be staggered ( $D_{5d}$ ) as in Fig. 19.27a and b since only this was compatible with the molecular inversion centre required by the crystallographic space group ( $C_{2h}^5$ ,  $Z = 2$ ). However, gas-phase electron diffraction data suggest that the equilibrium structure of ferrocene is eclipsed ( $D_{5h}$ ) as in Fig. 19.27c rather than staggered, with a rather low barrier to internal rotation of  $\sim 4 \text{ kJ mol}^{-1}$ . X-ray crystallographic<sup>(40)</sup> and neutron diffraction studies<sup>(41)</sup> confirm this general conclusion, the space-group symmetry requirement being met by a disordered arrangement of nearly eclipsed molecules (rotation angle between the rings  $\sim 9^\circ$  rather than  $0^\circ$  for precisely eclipsed or  $36^\circ$  for staggered conformation). Below 169 K the molecules become ordered, the rotation angle remaining  $\sim 9^\circ$ . The perpendicular distance between the rings is 325 pm (cf. graphite 335 pm) and the mean interatomic distances are Fe–C  $203 \pm 2$  pm and C–C  $139 \pm 6$  pm. The Ru and Os analogues  $[\text{M}(\eta^5\text{-C}_5\text{H}_5)_2]$  have similar molecular structures with eclipsed parallel  $\text{C}_5$  rings. A molecular-orbital description of the bonding can be developed along the lines indicated in

<sup>40</sup> P. SEILER and J. D. DUNITZ, *Acta Cryst.* **B35**, 1068–74 (1979).

<sup>41</sup> F. TAKUSAGAWA and T. F. KOETZLE, *Acta Cryst.* **B35**, 1074–81 (1979).

previous sections. Because of the importance of ferrocene, numerous calculations have been made of the detailed sequence of energy levels in the molecule; though these differ slightly depending on the assumptions made and the computational methods adopted, there is now a general consensus concerning the main features of the bonding as shown in the Panel.

A general preparative route to  $\eta^5\text{-C}_5\text{H}_5$  compounds is the reaction of  $\text{NaC}_5\text{H}_5$  with a metal halide or complex halide in a polar solvent such as thf,  $\text{Me}_2\text{O}$  (bp  $-23^\circ$ ),  $(\text{MeO})_2\text{C}_2\text{H}_4(\text{OMe})$ , or  $\text{HC(O)NMe}_2$ :



### A Molecular Orbital Description of the Bonding in $[\text{Fe}(\eta^5\text{-C}_5\text{H}_5)_2]$

The 5  $p_\pi$  atomic orbitals on the planar  $\text{C}_5\text{H}_5$  group can be combined to give 5 group MOs as shown in Fig. A; one combination has the full symmetry of the ring ( $a_1$ ) and there are two doubly degenerate combinations ( $e_1$  and  $e_2$ ) having respectively 1 and 2 planar nodes at right angles to the plane of the ring. These 5 group MOs can themselves be combined in pairs with a similar set from the second  $\text{C}_5\text{H}_5$  group before combining with metal orbitals. Each of the combinations [(ligand orbitals) + (metal orbitals)] leads, in principle, to a bonding MO of the molecule, providing that the energy of the two component sets is not very different. There are an equal number of antibonding combinations with the sign [(ligand orbitals) - (metal orbital)].

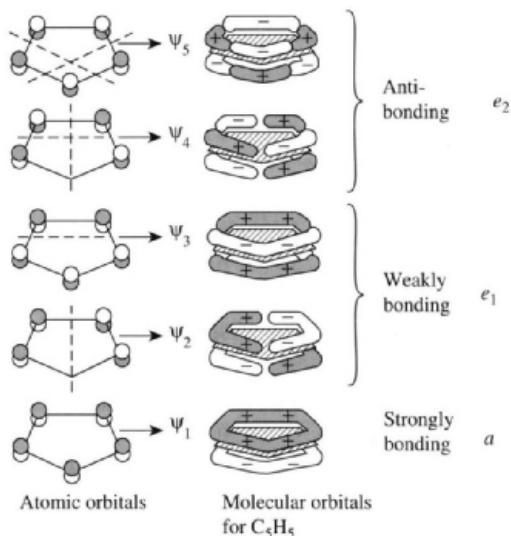


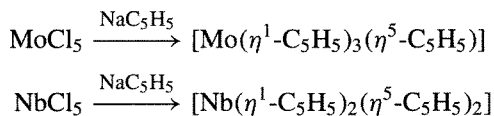
**Figure A** The  $\pi$  molecular orbitals formed from the set of  $p_\pi$  orbitals of the  $\text{C}_5\text{H}_5$  ring.

Calculation of the detailed sequence of energy levels arising from these combinations poses severe computational problems but a schematic indication of the sequence (not to scale) is shown in Fig. B. Thus, starting from the foot of the figure, the  $a_{1g}$  bonding MO is mainly ligand-based with only a slight admixture of the Fe 4s and  $3d_{z^2}$  orbitals. Similarly, the  $a_{2g}$  level has little, if any, admixture of the even higher-lying Fe  $4p_z$  orbital with which it is formally able to combine. The  $e_{1g}$  MO arises from the bonding combination of the ligand  $e_{1g}$  orbitals with Fe  $3d_{xz}$  and  $3d_{yz}$  and this is the main contribution to the stability of the complex; the corresponding antibonding  $e_{1g}^*$  are unoccupied in the ground state but will be involved in optical transitions. The  $e_{1u}$  bonding MOs are again mainly ligand-based but with some contribution from Fe  $4p_x$  and  $4p_y$ , etc. It can be seen that there is room for just 18 electrons in bonding and nonbonding MOs and that the antibonding MOs are unoccupied. In terms of electron counting the 18 electrons can be thought of as originating from the Fe atom (8e) and the two  $\text{C}_5\text{H}_5$  groups ( $2 \times 5e$ ) or from an  $\text{Fe}^{\text{II}}$  ion (6e) and two  $\text{C}_5\text{H}_5^-$  groups ( $2 \times 6e$ ).

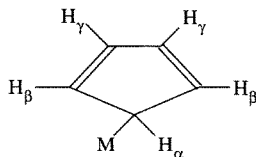
Panel continues



Innumerable derivatives have been synthesized in which one or more  $\eta^5$ -C<sub>5</sub>H<sub>5</sub> group is present in a mononuclear or polynuclear metal complex together with other ligands such as CO, NO, H or X. It should also be borne in mind that C<sub>5</sub>H<sub>5</sub> can act as an  $\eta^1$ -ligand by forming a  $\sigma$  M-C bond and mixed complexes are sometimes obtained, e.g. [Be( $\eta^1$ -C<sub>5</sub>H<sub>5</sub>)( $\eta^5$ -C<sub>5</sub>H<sub>5</sub>)] (see p. 130). Likewise:



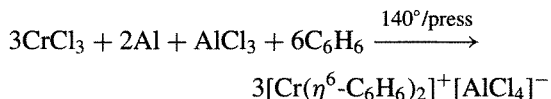
Such  $\eta^1$ -C<sub>5</sub>H<sub>5</sub> complexes are often found to be fluxional in solution at room temperature, the 5 H atoms giving rise to a single sharp <sup>1</sup>H nmr resonance. At lower temperatures the spectrum usually broadens and finally resolves into the expected complex spectrum at temperatures which are sufficiently low to prevent interchange on the nmr time scale ( $\sim 10^{-3}$  s). Numerous experiments have been devised to elucidate the mechanism by which the H atoms become equivalent and, at least in some systems, it seems likely that a non-dissociative (unimolecular) 1,2-shift occurs.



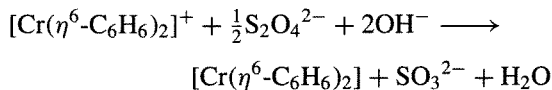
### 19.7.6 Hexahapto ligands

Arenes such as benzene and its derivatives can form complexes precisely analogous to ferrocene and related species. Though particularly exciting when first recognized as  $\eta^6$  complexes in 1955 these compounds introduce no new principles and need only be briefly considered here. Curiously, the first such compounds were made as long ago as 1919 when F. Hein reacted CrCl<sub>3</sub> with PhMgBr to give compounds which he formulated as "polyphenylchromium" compounds [CrPh<sub>n</sub>]<sup>0, +1</sup> ( $n = 2, 3, \text{ or } 4$ ); their true nature

as  $\eta^6$ -arene complexes of benzene and diphenyl was not recognized until over 35 y later.<sup>(43)</sup> The best general method for making bis( $\eta^6$ -arene) metal complexes is due to E. O. Fischer and W. Hafner (1955) who devised it originally for dibenzenechromium — the isoelectronic analogue of ferrocene: CrCl<sub>3</sub> was reduced with Al metal in the presence of C<sub>6</sub>H<sub>6</sub>, using AlCl<sub>3</sub> as a catalyst:

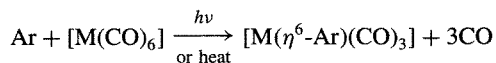


The yield is almost quantitative and the orange-yellow Cr<sup>I</sup> cation can be reduced to the neutral species with aqueous dithionite:



Dibenzenechromium(0) forms dark-brown crystals, mp 284°, and the molecular structure (Fig. 19.28) comprises plane parallel rings in eclipsed configuration above and below the Cr atom ( $D_{6h}$ ); the C-H bonds are tilted slightly towards the metal and, most significantly, the C-C distances show no alternation around the rings. A bonding scheme can be constructed as for ferrocene (p. 938) using the six p<sub>z</sub> orbitals on each benzene ring.

Bis ( $\eta^6$ -arene) metal complexes have been made for many transition metals by the Al/AlCl<sub>3</sub> reduction method and cationic species [M( $\eta^6$ -Ar)<sub>2</sub>]<sup>n+</sup> are also well established for  $n = 1, 2, \text{ and } 3$ . Numerous arenes besides benzene have been used, the next most common being 1,3,5-Me<sub>3</sub>C<sub>6</sub>H<sub>3</sub> (mesitylene) and C<sub>6</sub>Me<sub>6</sub>. Reaction of arenes with metal carbonyls in high-boiling solvents or under the influence of ultraviolet light results in the displacement of 3CO and the formation of arene-metal carbonyls:



<sup>43</sup> H. ZEISS, P. J. WHEATLEY and H. J. S. WINKLER, *Benzene-Metal Complexes*, Ronald Press, New York, 1966, 101 pp.

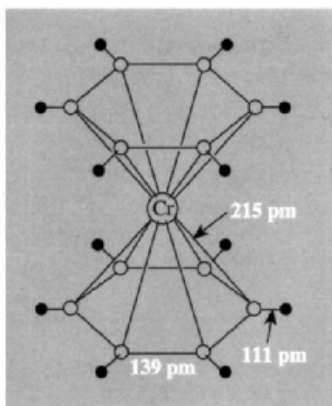


**Figure 19.28** The eclipsed ( $D_{6h}$ ) structure of  $[\text{Cr}(\eta^6\text{-C}_6\text{H}_6)_2]$  as revealed by X-ray diffraction, showing the two parallel rings 323 pm apart. Neutron diffraction shows the H atoms are tilted slightly towards the Cr, and electron diffraction on the gaseous compound shows that the eclipsed configuration is retained without rotation.

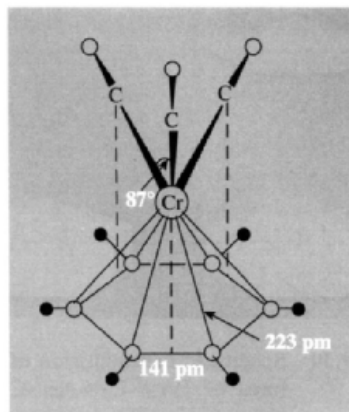
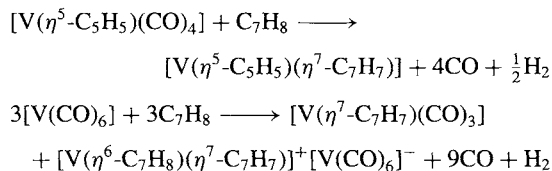


**Figure 19.29** The structure of  $[\text{Cr}(\eta^6\text{-C}_6\text{H}_6)(\text{CO})_3]$  showing the three CO groups in staggered configuration with respect to the benzene ring: the Cr–O distance is 295 pm and the plane of the 3 O atoms is parallel to the plane of the ring.

For Cr, Mo and W the benzenetricarbonyl complexes are yellow solids melting at  $162^\circ$ ,  $125^\circ$ , and  $140^\circ$ , respectively. The structure of  $[\text{Cr}(\eta^6\text{-C}_6\text{H}_6)(\text{CO})_3]$  is in Fig. 19.29. In general,  $\eta^6$ -arene complexes are more reactive than their  $\eta^5\text{-C}_5\text{H}_5$  analogues and are thermally less stable.

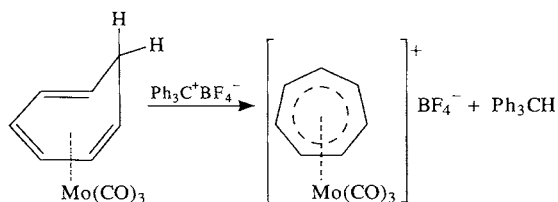
In some cases the loss of hydrogen may occur spontaneously, e.g.:



The purple paramagnetic complex  $[\text{V}(\eta^5\text{-C}_5\text{H}_5)(\eta^7\text{-C}_7\text{H}_7)]$  and the dark-brown diamagnetic complex  $[\text{V}(\eta^7\text{-C}_7\text{H}_7)(\text{CO})_3]$  both feature symmetrical planar  $\text{C}_7$  rings as illustrated in Fig. 19.30. The bonding appears to be similar to that in  $\eta^5\text{-C}_5\text{H}_5$  and  $\eta^6\text{-C}_6\text{H}_6$  complexes but, as expected from the large number of bonding electrons formally provided by the ligand, its complexes are restricted to elements in the early part of the transition series, e.g. V, Cr, Mo,  $\text{Mn}^{\text{I}}$ . For  $[\text{V}(\eta^5\text{-C}_5\text{H}_5)(\eta^7\text{-C}_7\text{H}_7)]$  the rings are “eclipsed” as shown, and a notable feature of the structure is the substantially closer approach of the  $\text{C}_7\text{H}_7$  ring to the V atom, suggesting that equality of V–C distances to the 2 rings is the controlling factor; consistent with this V–C(7 ring) is 225 pm and V–C(5 ring) is 223 pm. In addition to acting as an

### 19.7.7 Heptahapto and octahapto ligands

Treatment of cycloheptatriene complexes of the type  $[\text{M}(\eta^6\text{-C}_7\text{H}_8)(\text{CO})_3]$  ( $\text{M} = \text{Cr}, \text{Mo}, \text{W}$ ) with  $\text{Ph}_3\text{C}^+\text{BF}_4^-$  results in hydride abstraction to give orange-coloured  $\eta^7$ -cycloheptatrienyl (or tropylium) complexes:



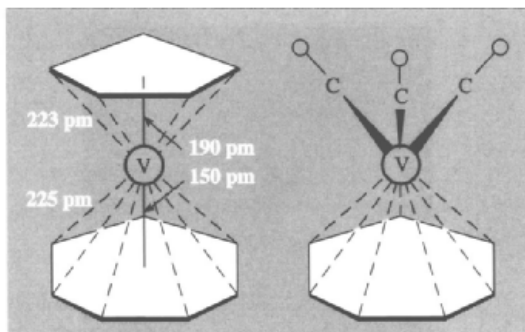


**Figure 19.30** Schematic representation of the structures of  $[\text{V}(\eta^5\text{-C}_5\text{H}_5)(\eta^7\text{-C}_7\text{H}_7)]$  and  $[\text{V}(\eta^7\text{-C}_7\text{H}_7)(\text{CO})_3]$  (see text).

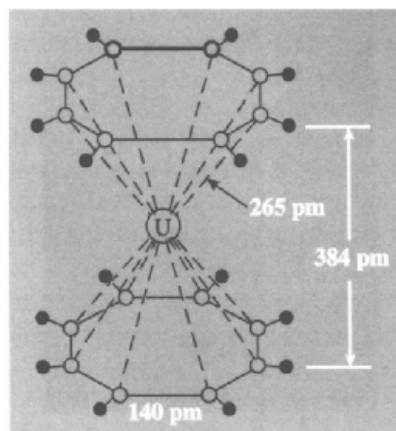
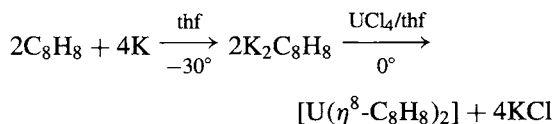


**Figure 19.31** The structure of  $[\text{U}(\eta^8\text{-C}_8\text{H}_8)_2]$  showing  $D_{8h}$  symmetry.

$\eta^7$  ligand, cycloheptatrienyl can also bond in the  $\eta^5, \eta^3$ , and even  $\eta^1$  mode (see ref. 44 on p. 943).

Octahapto ligands are rare but cyclooctatetraene fulfils this role in some of its complexes — the metal must clearly have an adequate number of unfilled orbitals and be large enough to bond effectively with such a large ring. Th, Pa, U, Np and Pu satisfy these criteria and the complexes  $[\text{M}(\eta^8\text{-C}_8\text{H}_8)_2]$  have been shown by X-ray crystallography to have eclipsed parallel planar rings (Fig. 19.31). The deep-green U complex can be made by reducing  $\text{C}_8\text{H}_8$  with K in dry thf and then reacting the intense yellow

solution of  $\text{K}_2\text{C}_8\text{H}_8$  with  $\text{UCl}_4$ :



The compound inflames in air but is stable in aqueous acid or alkali solutions. The colourless complex  $[\text{Th}(\eta^8\text{-C}_8\text{H}_8)_2]$ , yellow complexes  $[\text{Pa}(\eta^8\text{-C}_8\text{H}_8)_2]$  and  $[\text{Np}(\eta^8\text{-C}_8\text{H}_8)_2]$  and the cherry red compound  $[\text{Pu}(\eta^8\text{-C}_8\text{H}_8)_2]$  are prepared similarly. One of the very few

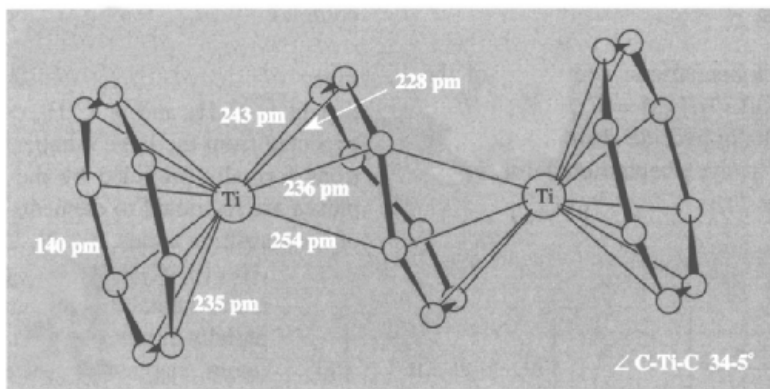


**Figure 19.32** Structure of  $[\text{Ti}_2(\text{C}_8\text{H}_8)_3]$  showing it to be  $[(\text{Ti}(\eta^8\text{-C}_8\text{H}_8))_2\mu\text{-}(\eta^4, \eta^4\text{-C}_8\text{H}_8)]$ . Ti-C to outer 16C = 235 pm. H atoms are omitted for clarity.

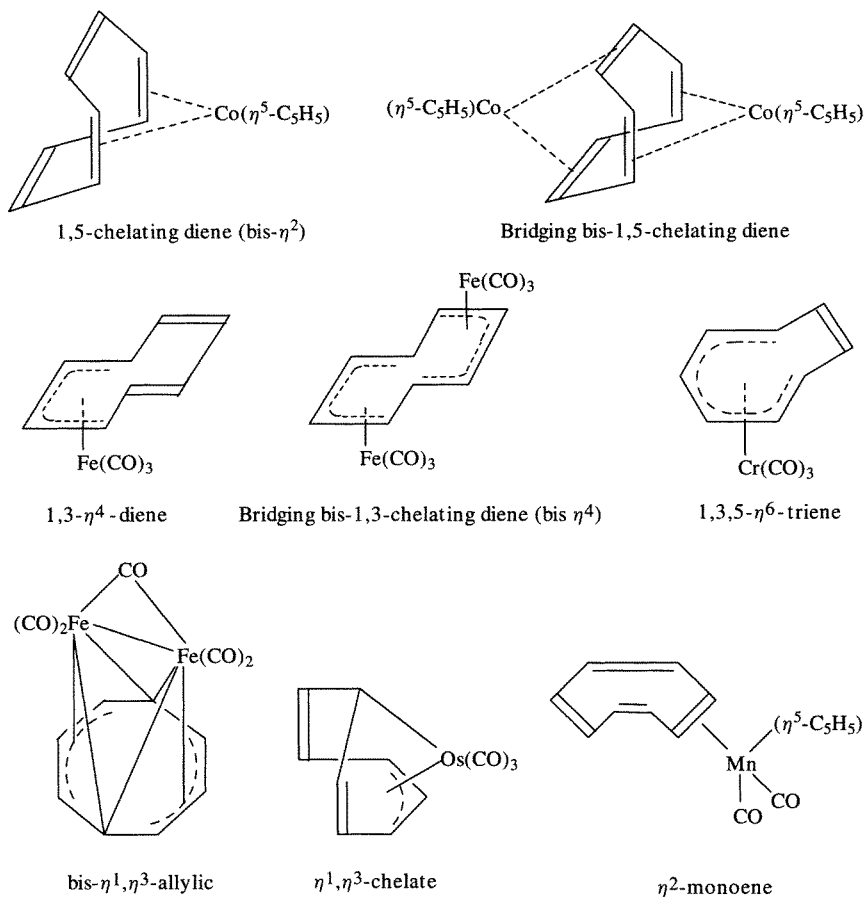


**Figure 19.33** Some further coordinating modes of  $C_8H_8$ .

examples of  $\eta^8$  bonding to a d-block element is in the curious complex  $Ti_2(C_8H_8)_3$ . As shown in Fig. 19.32, two of the ligands are planar  $\eta^8$  donors whereas the central puckered ring bridges the 2 Ti atoms in a bis- $\eta^4$ -mode. It is made by treating  $Ti(OBu^t)_4$  with  $C_8H_8$  in the presence of  $AlEt_3$ .

In addition to acting as an  $\eta^8$  ligand,  $C_8H_8$  can coordinate in other modes,<sup>(44)</sup> some of which are illustrated in Fig. 19.33. Many of these complexes show fluxional behaviour<sup>(45)</sup> in solution (p. 935) and the distinction between the various types of bonding is not as clear-cut as implied by the limiting structures in Fig. 19.33.

<sup>44</sup>G. DEGANELLO, *Transition Metal Complexes of Cyclic Polyolefins*. Academic Press, London, 1980, 476 pp.

<sup>45</sup>D. M. HEINEKEY and W. A. G. GRAHAM, *J. Am. Chem. Soc.* **101**, 6115–6 (1979).